PERGAMON

International Journal of Solids and Structures 40 (2003) 5769–5779

INTERNATIONAL JOURNAL OF SOLIDS and STRUCTURES

www.elsevier.com/locate/ijsolstr

Influence of plasticity on interface toughness in a layered solid with residual stresses

Viggo Tvergaard *

Department of Mechanical Engineering, Solid Mechanics, Technical University of Denmark, Building 404, DK-2800 Kgs. Lyngby, Denmark

Received 24 January 2003; received in revised form 12 June 2003

Abstract

For crack growth along an interface between two adjacent elastic–plastic materials in a layered solid, the resistance curve behaviour is analysed by approximating the behaviour in terms of a bi-material interface under small scale yielding conditions. Thus, it is assumed that the layers are thick enough so that the extent of the plastic regions around the crack tip are much smaller than the thickness of the nearest layers. The focus is on the effect of initial residual stresses in the layered material, or on T-stress components induced during loading. The fracture process is represented in terms of a cohesive zone model. It is found that the value of the T-stress component in the softer material adjacent to the interface crack plays a dominant role, such that a negative value of this T-stress gives a significant increase of the interface fracture toughness, while a positive value gives a reduction of the fracture toughness.

Keywords: Crack tip plasticity; Fracture process; Elastic–plastic material; Cohesive zone

1. Introduction

Resistance curves for interface crack growth have been analysed for a number of cases by using a cohesive zone model to represent the fracture process, while the surrounding material is represented as elastic–plastic. Thus, Tvergaard and Hutchinson (1993) have studied crack growth between a ductile solid and a rigid solid, and Tvergaard (2001) has considered a crack between dissimilar elastic–plastic solids. These analyses for conditions of small scale yielding have accounted for mixed mode loading on the solid, and it has been found that a significant contribution of mode II loading at the crack tip gives much higher fracture toughness than that found when mode I loading dominates at the crack tip, in good agreement with experimental observations (Cao and Evans, 1989; Liechti and Chai, 1992; O'Dowd et al., 1992).

The effect of a residual stress parallel to the crack plane has been studied by Tvergaard and Hutchinson (1996) in an analysis of crack propagation along one of the interfaces between a thin ductile adhesive layer and the elastic substrates that it joins. Related to this is the analysis of crack growth in a homogeneous solid

* Tel.: +45-4525-4273; fax: +45-4593-1475.
E-mail address: viggo@mek.dtu.dk (V. Tvergaard).

0020-7683/$ - see front matter © 2003 Elsevier Ltd. All rights reserved.
doi:10.1016/S0020-7683(03)00342-1

with a T-stress (Tvergaard and Hutchinson, 1994a,b), which has shown that the model using a cohesive zone in an elastic–plastic solid predicts the strongly increased fracture toughness in the presence of a negative T-stress, that has been shown by experiments for homogeneous specimens under mode I loading (Hancock et al., 1991), where the magnitude of the T-stress depends strongly on the specimen type and geometry. Recently, Tvergaard (2002) has analysed the more idealised problem of crack growth along an interface between an elastic–plastic solid and an elastic solid, where only a T-stress in the elastic–plastic solid is accounted for. This preliminary study has shown that a stress component parallel to the interface crack plane has a significant effect on the fracture toughness.

In the present analyses the materials on both sides of the interface are represented as elastic–plastic, and stress components parallel to the interface crack plane are accounted for in both materials. The analyses, carried out for an interface crack growing between two different materials, is considered a good approximation for a layered material as long as the layer thickness is much larger than the extent of the plastic region at the crack tip. If the stresses parallel to the interface crack plane result from thermal contraction mismatch between the layers, the signs of the stresses are opposite in neighbouring layers, and the relative magnitudes of the stresses depend on the ratios of the layer thicknesses. The stresses can also result from the specimen type and geometry, as is common for usual T-stresses, and the stresses can arise from a combination of these effects. If the stress components in the crack growth direction result from thermal contraction mismatch, these stress components are equal to the transverse stresses, whereas the transverse stresses are smaller for usual T-stresses, as resulting from plane strain conditions. Both levels of transverse stresses are considered here, to show that the results differ only little. A parametric study is carried out for a wide variety of ratios between the stresses in adjacent layers, as can result from residual stresses with different ratios of the layer thicknesses, from T-stress effects, or from combinations of these.

2. Problem formulation

In the layered solid it is assumed that the layers are thick enough so that the extent of the plastic regions around the interface crack tip are much smaller than the thickness of the nearest layer. Then, the problem can be well approximated by a small scale yielding analysis for a crack growing between two different materials, as illustrated in Fig. 1, where each material layer has initial residual stresses.

The elastic interface crack problem was solved long ago by many authors (e.g. England, 1965). Following the formulation of Rice (1988) (see also Tvergaard and Hutchinson, 1993), the crack has tractions

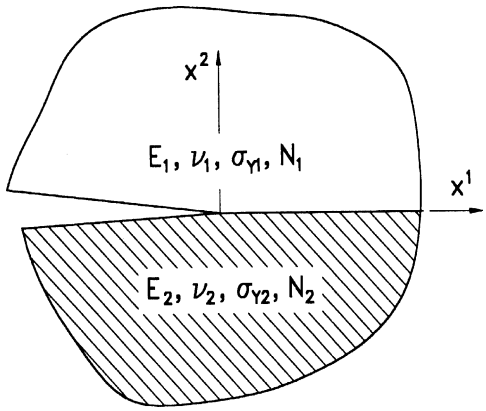

Fig. 1. Interface crack between two material layers, with different elastic–plastic properties in each material.

acting on the interface, which are given in terms of the two stress intensity factor components, K_{I} and K_{II}, by

$$\sigma_{22}+\mathrm{i}\sigma_{12}=(K_{\mathrm{I}}+\mathrm{i}K_{\mathrm{II}})(2\pi r)^{-1/2}r^{\mathrm{i}\varepsilon} \tag{2.1}$$

Here, r is the distance from the tip, $\mathrm{i}=\sqrt{-1}$, ε is the oscillation index

$$\varepsilon=\frac{1}{2\pi}\ln\left(\frac{1-\beta}{1+\beta}\right) \tag{2.2}$$

and β is the second Dundurs' parameter

$$\beta=\frac{1}{2}\frac{\mu_1(1-2\nu_2)-\mu_2(1-2\nu_1)}{\mu_1(1-\nu_2)+\mu_2(1-\nu_1)} \tag{2.3}$$

where the shear moduli are $\mu_1=E_1/(2(1+\nu_1))$ and $\mu_2=E_2/(2(1+\nu_2))$. The relation between the energy release rate and the magnitude $|K|$ of stress intensity factors is

$$G=\frac{1}{2}(1-\beta^2)\left[\frac{1-\nu_1^2}{E_1}+\frac{1-\nu_2^2}{E_2}\right]|K|^2,\quad |K|=\sqrt{K_{\mathrm{I}}^2+K_{\mathrm{II}}^2} \tag{2.4}$$

With a reference length L chosen to characterize the remote field, an L-dependent measure of mode mixity ψ is defined by

$$\tan\psi=\frac{\mathrm{Im}[(K_{\mathrm{I}}+\mathrm{i}K_{\mathrm{II}})L^{\mathrm{i}\varepsilon}]}{\mathrm{Re}[(K_{\mathrm{I}}+\mathrm{i}K_{\mathrm{II}})L^{\mathrm{i}\varepsilon}]} \tag{2.5}$$

which reduces to the more familiar measure, $\tan\psi=K_{\mathrm{II}}/K_{\mathrm{I}}$, when $\varepsilon=0$. The displacement components associated with the singularity field, with amplitude $|K|$, are specified in Tvergaard and Hutchinson (1993).

The small strain linear elastic solution for the in-plane stress components containing the oscillating singularity in r are denoted $\Sigma_{\alpha\beta}(r,\theta)$, as partly described by (2.1). With the effect of a T-stress, the in-plane stresses near the crack tip are taken to be of the form

$$\sigma_{\alpha\beta}=\Sigma_{\alpha\beta}(r,\theta)+T\delta_{1\alpha}\delta_{1\beta} \tag{2.6}$$

where (r,θ) are polar coordinates and δ_{ij} is Kronecker's delta. The second term in (2.6) gives the non-singular T-stress, which can result from residual stresses due to the thermal contraction mismatch of the two materials joined at the interface, as studied by Tvergaard and Hutchinson (1996). Alternatively, the T-stress can result from the specimen type and geometry, as described in Hancock et al. (1991). In the latter case the T-stress applied under plane strain conditions will result in a transverse stress $\sigma_{33}=\nu T$, whereas the corresponding transverse stress will be $\sigma_{33}=T$ if the T-stress results from thermal contraction mismatch between the layers. In the case of self-equilibrating residual stresses, the sign of the stresses will be opposite in the two types of layers and their relative magnitude will depend on the ratio of the layer thicknesses. Most analyses here will consider $\sigma_{33}=\nu T$, but some results for $\sigma_{33}=T$ are included to show that this does not make much difference. The values of the T-stresses in the two material layers adjacent to the crack are denoted T_1 and T_2, respectively.

Both material no. 1, above the cracked interface, and material no. 2, below the interface, are taken to be elastic–plastic, with the true stress–logarithmic strain curve in uniaxial tension specified by

$$\varepsilon=\begin{cases}\sigma/E & \text{for } \sigma\leqslant\sigma_{\mathrm{Y}}\\ (\sigma_{\mathrm{Y}}/E)(\sigma/\sigma_{\mathrm{Y}})^{1/N} & \text{for } \sigma\geqslant\sigma_{\mathrm{Y}}\end{cases} \tag{2.7}$$

Here, σ_{Y} is the initial yield stress and N is the power hardening exponent, while E and ν are Young's modulus and Poisson's ratio, respectively. The tensile behaviour is generalized to multiaxial stress states

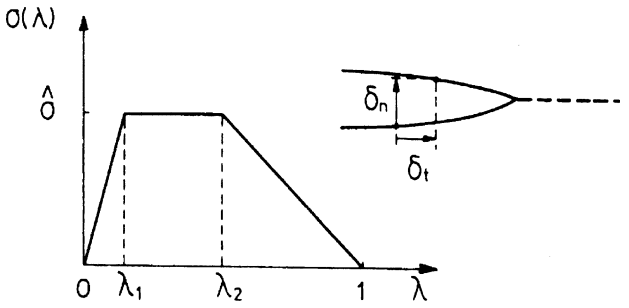

Fig. 2. Specification of traction–separation relation.

assuming isotropic hardening and using the Mises yield surface. For material no. 1 the parameters are denoted E_1, ν_1, σ_{Y1} and N_1, while material no. 2 has the material parameters E_2, ν_2, σ_{Y2} and N_2.

The fracture process is represented in terms of a cohesive zone model also used by Tvergaard and Hutchinson (1993), which is a special version of a traction–separation law proposed by Needleman (1987) and generalized by Tvergaard (1990). Here, δ_n and δ_t denote the normal and tangential components of the relative displacement of the crack faces across the interface in the zone where the fracture processes are occurring (Fig. 2), with critical values δ_n^c and δ_t^c. A single non-dimensional separation measure is defined as $\lambda = [(\delta_n/\delta_n^c)^2 + (\delta_t/\delta_t^c)^2]^{1/2}$, and the tractions drop to zero when $\lambda = 1$. With $\sigma(\lambda)$ displayed in Fig. 2, a potential from which the tractions are derived is defined as

$$\Phi(\delta_n, \delta_t) = \delta_n^c \int_0^\lambda \sigma(\lambda')\, d\lambda' \tag{2.8}$$

The normal and tangential components of the traction acting on the interface in the fracture process zone are given by

$$T_n = \frac{\partial \Phi}{\partial \delta_n} = \frac{\sigma(\lambda)}{\lambda}\frac{\delta_n}{\delta_n^c}, \qquad T_t = \frac{\partial \Phi}{\partial \delta_t} = \frac{\sigma(\lambda)}{\lambda}\frac{\delta_t}{\delta_t^c}\frac{\delta_n^c}{\delta_t^c} \tag{2.9}$$

The peak normal traction under pure normal separation is $\hat{\sigma}$, and the peak shear traction is $(\delta_n^c/\delta_t^c)\hat{\sigma}$ in a pure tangential separation. The work of separation per unit area of interface is given by Eq. (2.8) with $\lambda = 1$, and for the separation function $\sigma(\lambda)$ in Fig. 2 the work is

$$\Gamma_0 = \frac{1}{2}\hat{\sigma}\delta_n^c(1 - \lambda_1 + \lambda_2) \tag{2.10}$$

It has been found by Tvergaard and Hutchinson (1992, 1993) that the two most important parameters characterizing the fracture process in this model are Γ_0 and $\hat{\sigma}$, while the details of the shape of the separation law are less important.

On the free crack surfaces, for $x^2 = 0$ and $x^1 < 0$, zero tractions, $T^1 = T^2 = 0$, are prescribed, while on the remaining part of the interface, $x^2 = 0$ and $x^1 > 0$, the displacements and tractions are related by the traction–separation law (2.9).

Based on (2.4) and (2.10) a reference stress intensity factor is defined as

$$K_0 = \left[\frac{1-\nu_1^2}{E_1} + \frac{1-\nu_2^2}{E_2}\right]^{-1/2}\left(\frac{2\Gamma_0}{1-\beta^2}\right)^{1/2} \tag{2.11}$$

Here, K_0 represents the value of $|K|$ needed to advance the interface crack in the absence of any plasticity. This value is independent of ψ since a potential is used to generate the relation of tractions to crack face

displacements of the interface. A length quantity R_0, which scales with the size of the plastic zone in material no. 1 (when $|K| \cong K_0$), is defined as

$$R_0 = \frac{1}{3\pi}\left(\frac{K_0}{\sigma_{Y1}}\right)^2 = \frac{2}{3\pi}\left[\frac{1-\nu_1^2}{E_1}+\frac{1-\nu_2^2}{E_2}\right]^{-1}\frac{\Gamma_0}{(1-\beta^2)\sigma_{Y1}^2} \tag{2.12}$$

While the mode mixity measure ψ refers to the distance L from the tip, it is natural to define a reference measure of mixity, ψ_0, based on the reference length R_0. The relation between ψ_0 and ψ is

$$\psi_0 = \psi + \varepsilon \ln(R_0/L) \tag{2.13}$$

3. Numerical solution

In the numerical analyses finite strains are accounted for, using a convected coordinate, Lagrangian formulation of the field equations, in which g_{ij} and G_{ij} are metric tensors in the reference configuration and the current configuration, respectively, with determinants g and G, and $\eta_{ij} = 1/2(G_{ij} - g_{ij})$ is the Lagrangian strain tensor. The contravariant components τ^{ij} of the Kirchhoff stress tensor on the current base vectors are related to the components of the Cauchy stress tensor σ^{ij} by $\tau^{ij} = \sqrt{G/g}\,\sigma^{ij}$. Then, in the finite strain generalization of J_2-flow theory discussed by Hutchinson (1973), an incremental stress–strain relationship is obtained of the form $\dot{\tau}^{ij} = L^{ijkl}\dot{\eta}_{kl}$ (e.g. see Tvergaard and Hutchinson, 1993).

The numerical solutions are obtained by a crack growth procedure as that used by Tvergaard and Hutchinson (1993) and Tvergaard (2001). Thus, a finite element approximation of the displacement fields is used in a linear incremental method, with a Cartesian coordinate system x^i as reference. The solution is based on the incremental principle of virtual work, with equilibrium correction terms applied. First the non-singular T-stresses and the corresponding transverse stress components in the x^3-direction are applied, considering only T-stress levels well below those resulting in plastic yielding. Subsequently, the singular part

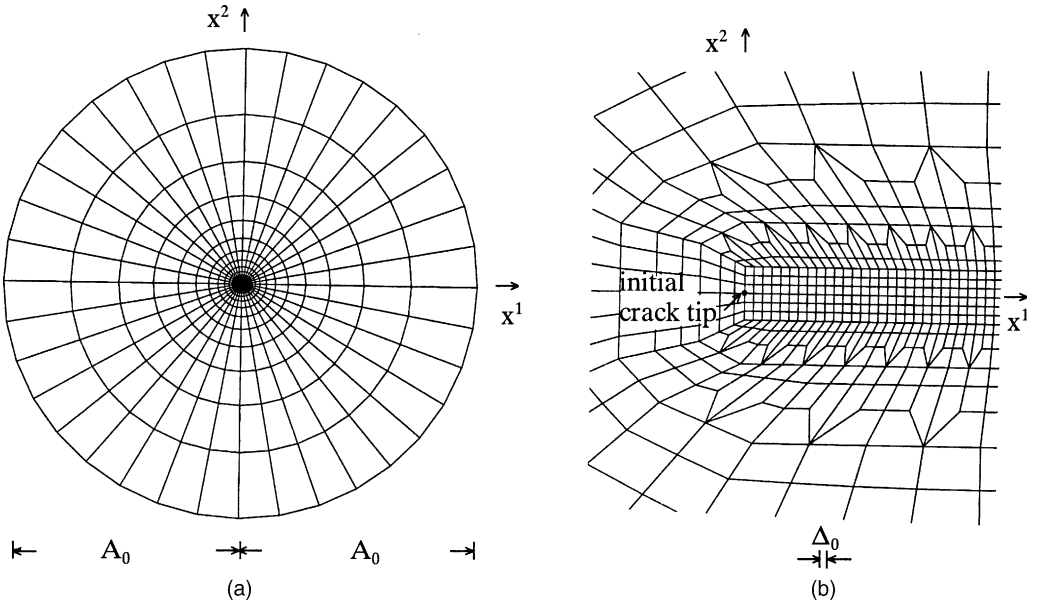

Fig. 3. Mesh used for some of the crack growth analyses.

of the solution is applied incrementally by prescribing the appropriate displacement increments on the outer boundary of the region analysed. During the initial part of the crack growth resistance curve an increment of $|K|$ is prescribed, but when $|K|$ approaches its asymptote, a Rayleigh–Ritz finite element method (Tvergaard, 1976) is needed to ensure a monotonic increase in displacement differences across the crack tip. It is noted that full finite strain effects are accounted for so that crack tip blunting can be represented, and this is important if the peak stress $\hat{\sigma}$ of the debonding model is near or above the maximum possible stress during blunting.

An example of the mesh used for the computations is shown in Fig. 3. A uniform mesh region is used in the range where crack growth is studied. The length of one square element inside the uniform mesh is denoted Δ_0, and the initial crack tip is located at $x^1 = 0$. The computations are carried out with 120×6 quadrilaterals in the uniform mesh along the interface. The elements used are quadrilaterals each built-up of four triangular, linear-displacement elements. The outer radius of the region analysed is chosen to be $A_0/\Delta_0 = 80\,000$, in order that the plastic zone size should not exceed $A_0/10$. The J-integral (Rice, 1968; Eshelby, 1970) is calculated at some stages of the deformation, to check agreement with the prescribed value of $|K|$.

4. Results

In the analyses to be presented here the values of the material parameters for material no. 1 are taken to be $\sigma_{Y1}/E_1 = 0.003$, $\nu_1 = 1/3$ and $N_1 = 0.1$. For material no. 2 different values of the ratios E_2/E_1 and σ_{Y2}/σ_{Y1} are considered, while $\nu_2 = 1/3$ and $N_2 = 0.1$ are kept fixed. In the traction–separation law the values $\delta_n^c/\delta_t^c = 1$, $\delta_n^c = 0.1\Delta_0$, $\lambda_1 = 0.15$ and $\lambda_2 = 0.50$ are used, and the peak stress is taken to be $\hat{\sigma} = 4.0\sigma_{Y1}$.

Computed crack growth resistance curves are shown in Fig. 4 for $E_2/E_1 = 2.0$ and $\sigma_{Y2}/\sigma_{Y1} = 2$ in cases where the mode mixity near the crack tip is specified by $\psi_0 = 3.95°$, and where the transverse stress is $\sigma_{33} = \nu T$. It is seen that the values of the T-stresses have a very strong influence on the development of the fracture toughness $|K|_R$ with the growth Δa of the crack length. For $T_1/\sigma_{Y1} = -0.5$ and $T_2/\sigma_{Y1} = 0.5$ the

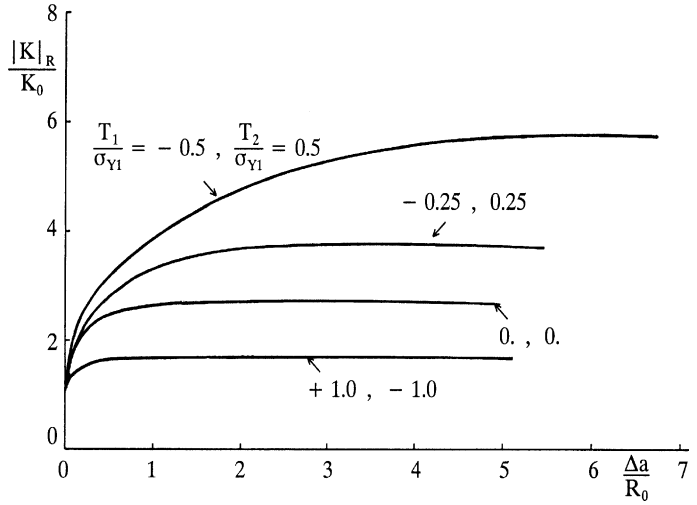

Fig. 4. Interface crack growth resistance curves for various values of $T_1 = -T_2$, with $\sigma_{Y1}/E_1 = 0.003$, $\hat{\sigma}/\sigma_{Y1} = 4.0$, $E_2/E_1 = 2$, $\sigma_{Y2}/\sigma_{Y1} = 2$, $\sigma_{33} = \nu T$ and $\psi_0 = 3.95°$.

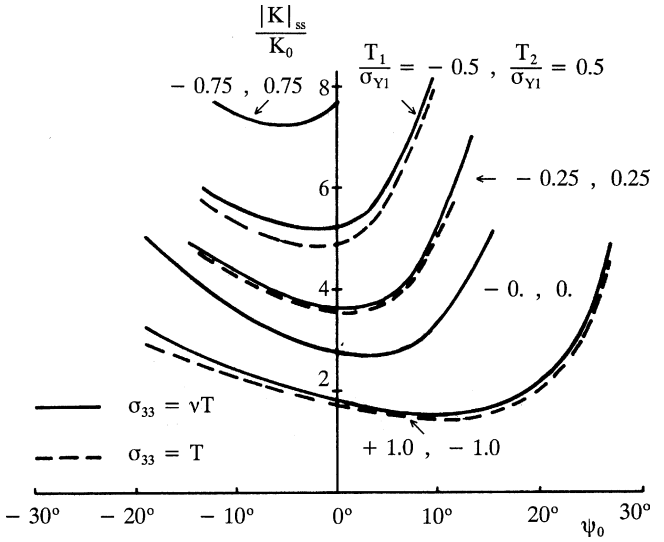

Fig. 5. Steady-state interface toughness as a function of the local mixity measure ψ_0 for various values of $T_1 = -T_2$, with $\sigma_{Y1}/E_1 = 0.003$, $\hat{\sigma}/\sigma_{Y1} = 4.0$, $E_2/E_1 = 2$ and $\sigma_{Y2}/\sigma_{Y1} = 2$.

fracture toughness grows much larger than that found for $T_1 = T_2 = 0$, and for $T_1/\sigma_{Y1} = 1.0$ and $T_2/\sigma_{Y1} = -1.0$ the toughness is noticeably smaller.

Curves of the steady-state fracture toughness $|K|_{ss}/K_0$ vs. ψ_0 are shown in Fig. 5 to illustrate the dependence on the mode-mixity. The material parameters here are the same as those considered in Fig. 4, and again the different curves correspond to different levels of the T-stresses. The solid curves are obtained by taking the transverse stress to be $\sigma_{33} = \nu T$, and the points for $\psi_0 = 3.95°$ on these curves are equal to the peak values of the resistance curves shown in Fig. 4. The dashed curves in Fig. 5 are obtained by prescribing the transverse stress $\sigma_{33} = T$. For all the curves in Fig. 5 the T-stresses in the two materials are taken to be of opposite sign, but of equal absolute magnitude, as in Fig. 4. Material no. 1, with the lower initial yield stress, experiences a much larger plastic zone than that in material no. 2, and therefore a negative T-stress in material no. 1 gives a significant increase of the fracture toughness, while a negative T-stress in material no. 2 does not have this effect. It is noted that the dashed curves in Fig. 5 are a little below the solid curves, so that the value $\sigma_{33} = T$ for the transverse stress gives slightly lower fracture toughness, but the main conclusion here is that there is only little sensitivity to the different levels of σ_{33}/T considered here.

The resistance curves for $\sigma_{33} = T$ were not shown in Fig. 4. But it is noted that they closely follow the corresponding solid curves in Fig. 4 (for $\sigma_{33} = \nu T$), falling slightly below in agreement with the difference of the steady-state values at $\psi_0 = 3.95°$ specified in Fig. 5.

The characteristic feature found in previous studies of interface crack growth (Tvergaard and Hutchinson, 1993; Tvergaard, 2001) that the minimum fracture toughness occurs at $\psi_0 \cong 0°$, i.e. for mode I conditions near the crack tip, is also seen in Fig. 5 for $T_1 = T_2 = 0$. Furthermore, as also found before, a noticeable mode II contribution results in much increased fracture toughness. The same general characteristics are found for all the curves in Fig. 5, but the minimum shifts towards negative values of ψ_0 for increasing negative values of T_1, while the minimum for $T_1/\sigma_{Y1} = 1.0$ has shifted to the positive value, $\psi_0 \cong 10°$. It is noted that these features are rather similar to results found recently for an elastic–plastic solid with a T-stress bonded to an elastic substrate with very high stiffness (Tvergaard, 2002).

The curves in Fig. 6 have been determined to obtain a parametric understanding of the effect of varying the values of T_1 and T_2 relative to each others. These computations are carried out for $\psi_0 = 3.95°$ and for $\sigma_{33} = \nu T$, and the corresponding point on the curve for $T_1/\sigma_{Y1} = -0.5$ and $T_2/\sigma_{Y1} = 0.5$ in Fig. 5 appears

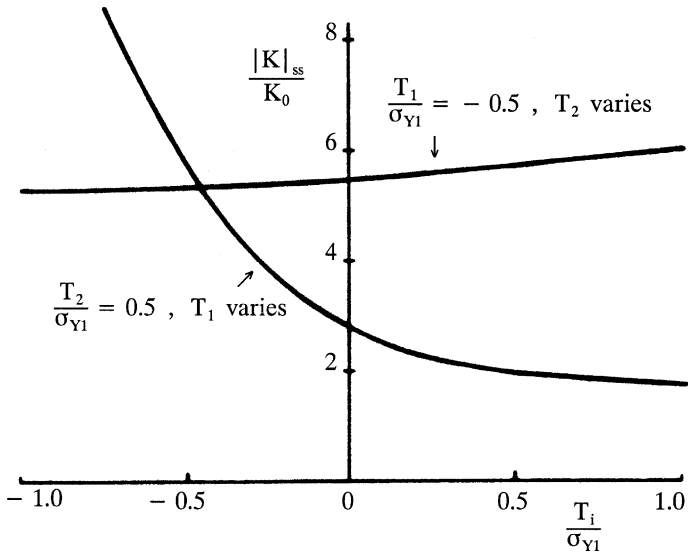

Fig. 6. Steady-state interface toughness for $\psi_0 = 3.95°$, and for T_2 varying with $T_1/\sigma_{Y1} = -0.5$ or for T_1 varying with $T_2/\sigma_{Y1} = 0.5$. Interface characterized by $\sigma_{Y1}/E_1 = 0.003$, $\hat{\sigma}/\sigma_{Y1} = 4.0$, $E_2/E_1 = 2$ and $\sigma_{Y2}/\sigma_{Y1} = 2$, with $\sigma_{33} = \nu T$.

on both curves in Fig. 6. However, one of the curves in Fig. 6 keeps $T_2/\sigma_{Y1} = 0.5$ fixed, while T_1 is varied, and the other curve keeps $T_1/\sigma_{Y1} = -0.5$ fixed, while T_2 is varied. The latter curve shows rather little sensitivity to variations of the value of T_2, since the plastic zone in material no. 2, affected by T_2, is much smaller than that in material no. 1. On the other hand, the curve where T_1 is varied shows a strong sensitivity to these variations, as should be expected since the value of T_1 has a strong influence on the size of the plastic region in the softer material.

The curves in Fig. 7 show the steady-state fracture toughness $|K|_{ss}/K_0$ vs. ψ_0 for cases where $E_2/E_1 = 1$ and $\sigma_{Y2}/\sigma_{Y1} = 1.5$, with $\hat{\sigma}/\sigma_{Y1} = 4.0$. As in Fig. 5 the values of the T-stresses in the two materials are taken

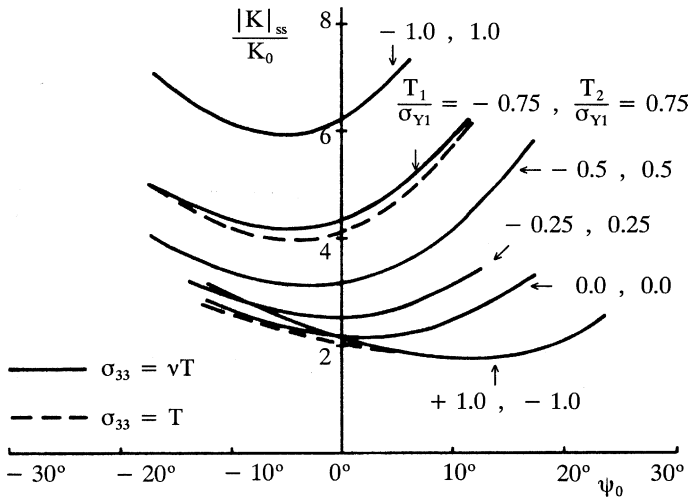

Fig. 7. Steady-state interface toughness as a function of the local mixity measure ψ_0 for various values of $T_1 = -T_2$, with $\sigma_{Y1}/E_1 = 0.003$, $\hat{\sigma}/\sigma_{Y1} = 4.0$, $E_2/E_1 = 1$ and $\sigma_{Y2}/\sigma_{Y1} = 1.5$.

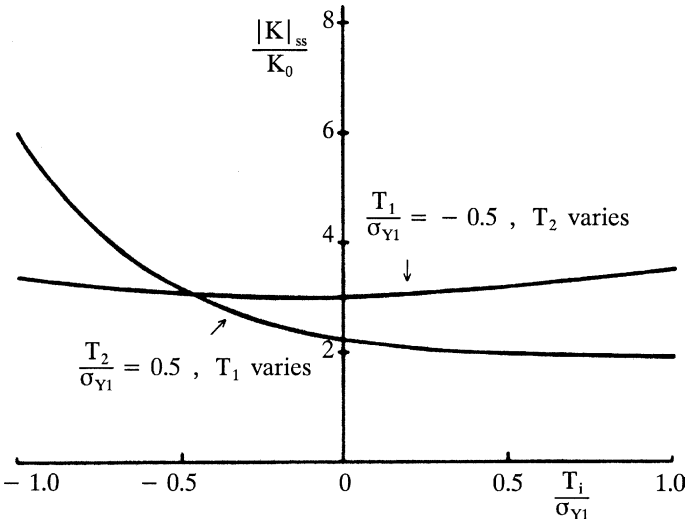

Fig. 8. Steady-state interface toughness for $\psi_0 = 0°$, and for T_2 varying with $T_1/\sigma_{Y1} = -0.5$ or for T_1 varying with $T_2/\sigma_{Y1} = 0.5$. Interface characterized by $\sigma_{Y1}/E_1 = 0.003$, $\hat{\sigma}/\sigma_{Y1} = 4.0$, $E_2/E_1 = 1$ and $\sigma_{Y2}/\sigma_{Y1} = 1.5$, with $\sigma_{33} = \nu T$.

to be of opposite sign, but of equal absolute magnitude. The curves show the same trends as those in Fig. 5 that the minima occur in the vicinity of $\psi_0 = 0°$, and that the steady-state fracture toughness increases significantly when a noticeable mode II contribution is applied. Also, the location of the minimum shifts towards a negative value of ψ_0 when $T_1 < 0$, while a positive value of T_1 shifts the location of the minimum to a positive ψ_0. The solid curves in Fig. 7 correspond to taking the transverse stress as $\sigma_{33} = \nu T$, while the two examples of dashed curves correspond to $\sigma_{33} = T$. As in Fig. 5 it is seen that the fracture toughness shows only a slight sensitivity to the difference in the level of σ_{33}/T considered here.

Fig. 8 shows the effect of varying the values of T_1 and T_2 relative to each others, analogous to Fig. 6. Even though the initial yield stress in material no. 2 is here only 1.5 times that in material no. 1, the plastic zone is still much smaller in the substrate than in material no. 1. Therefore, the effect of varying T_1 for a fixed value $T_2/\sigma_{Y1} = 0.5$ is also here much larger than the effect of varying T_2 for a fixed value $T_1/\sigma_{Y1} = -0.5$.

5. Discussion

The present studies for crack growth along an interface between two elastic–plastic materials in a layered material consider a wide variety of combinations of the initial stresses in the material layers. These stresses parallel to the interface plane, on which the crack is assumed to grow, can result from thermal contraction mismatch, with the stress ratios dependent on the ratio of the layer thicknesses, or from T-stresses that depend on the specimen type and crack depth, or from a combination of these, and therefore several combinations of the initial stress values are of interest. Since the analyses are actually carried out for a bi-material interface under conditions of small scale yielding, the approximation to a layered material is only reasonable as long as the plastic region around the crack tip is much smaller than the thickness of the layer in which it is contained.

The largest part of the plastic region at the crack tip occurs in the neighbouring layer that has the lowest yield stress, and the T-stress component in this layer has a strong influence on the size of the plastic region in the layer. Therefore, the results in the present paper show much similarity with resistance curve behaviour found for crack growth in a homogeneous solid with a T-stress (Tvergaard and Hutchinson,

1994a,b), when comparison is made with values of the T-stress component in the more ductile layer, i.e. T_1 in the present paper. Thus, a negative value of the ratio T_1/σ_{Y1}, approaching -1.0, gives a significant increase of the fracture toughness, even if T_2 is positive. On the other hand, a positive value of T_1 gives some reduction of the fracture toughness, which was not found for a homogeneous solid with a T-stress. A similar effect of a positive T_1 was found in a recent study for a crack growing between an elastic–plastic solid and a very stiff elastic substrate.

Much focus has been given here to the fact that the non-singular stress components parallel to the crack plane can have different origins. In a layered material such residual stresses would typically arise from thermal contraction mismatch during cooling from the processing temperature, which would give stresses of opposite sign in neighbouring layers. In that case the transverse residual stresses in the direction parallel to the crack front are equal to the residual stress component in the crack growth direction in the same material layer. On the other hand, when the T-stresses arise from the specimen type and geometry, during loading, the transverse stresses are smaller. The results in the present paper show that the resistance curve behaviour and the steady-state interface fracture toughness are not very sensitive to these differences in the transverse stress.

A wide variety of combinations of the T-stresses, T_1 and T_2, in adjacent material layers has been considered in Figs. 6 and 8, by keeping the stress component in one of the material layers fixed while that in the other material is varied. These analyses have been carried out for values of the mode mixity parameter ψ_0 near 0°, so that the stress-state in the near vicinity of the crack tip is close to pure mode I loading. These studies show that the interface fracture toughness is strongly affected by variations of the ratio T_1/σ_{Y1} in the softer material when the value of T_2 is kept fixed. On the other hand, the figures also show that when the value of T_1 is kept fixed, there is quite low sensitivity to variations of the stress component T_2 in the harder material layer.

A noticeable feature of the curves on Figs. 5 and 7, showing the dependence of the interface fracture toughness on the mode mixity, is that for a negative value of the T-stress in the softer material the minimum of the fracture toughness moves towards a negative value of ψ_0, while for a positive value of the T-stress in the softer material the minimum moves towards a positive value of ψ_0. From previous investigations it was already known that in the absence of a T-stress the minimum of the fracture toughness occurs in the vicinity of $\psi_0 = 0°$.

References

Cao, H.C., Evans, A.G., 1989. An experimental study of the fracture resistance of bimaterial interfaces. Mech. Mater. 7, 295–304.

England, A.H., 1965. A crack between dissimilar media. J. Appl. Mech. 32, 400–402.

Eshelby, J.D., 1970. In: Kanninen, M.F. et al. (Eds.), Inelastic Behavior of Solids. McGraw-Hill, New York, pp. 77–115.

Hancock, J.W., Reuter, W.G., Parks, D.M., 1991. Constraint and toughness parameterised by T. In: ASTM Symposium on Constraint Effects in Fracture, Indianapolis.

Hutchinson, J.W., 1973. Finite strain analysis of elastic–plastic solids and structures. In: Hartung, R.F. (Ed.), Numerical Solution of Nonlinear Structural Problems. ASME, New York, p. 17.

Liechti, K.M., Chai, Y.S., 1992. Asymmetric shielding in interfacial fracture under in-plane shear. J. Appl. Mech. 59, 295.

Needleman, A., 1987. A continuum model for void nucleation by inclusion debonding. J. Appl. Mech. 54, 525–531.

O'Dowd, N.P., Stout, M.G., Shih, C.F., 1992. Fracture toughness of alumina/niobium interfaces: experiments and analyses. Phil. Mag. A 66, 1037.

Rice, J.R., 1968. A path independent integral and the approximate analysis of strain concentration by notches and cracks. J. Appl. Mech. 35, 379–386.

Rice, J.R., 1988. Elastic fracture mechanics concepts for interfacial cracks. J. Appl. Mech. 55, 98–103.

Tvergaard, V., 1976. Effect of thickness inhomogeneities in internally pressurized elastic–plastic spherical shells. J. Mech. Phys. Solids 24, 291–304.

Tvergaard, V., 1990. Effect of fibre debonding in a whisker-reinforced metal. Mater. Sci. Engng. A 125, 203–213.

Tvergaard, V., 2001. Resistance curves for mixed mode interface crack growth between dissimilar elastic–plastic solids. J. Mech. Phys. Solids 49, 2689–2703.
Tvergaard, V., 2002. Effect of T-stress on crack growth along an interface between ductile and elastic solids. Department of Mechanical Engineering, Solid Mechanics, Report.
Tvergaard, V., Hutchinson, J.W., 1992. The relation between crack growth resistance and fracture process parameters in elastic–plastic solids. J. Mech. Phys. Solids 40, 1377–1397.
Tvergaard, V., Hutchinson, J.W., 1993. The influence of plasticity on mixed mode interface toughness. J. Mech. Phys. Solids 41, 1119–1135.
Tvergaard, V., Hutchinson, J.W., 1994a. Effect of T-stress on mode I crack growth resistance in a ductile solid. Int. J. Solids Struct. 31, 823–833.
Tvergaard, V., Hutchinson, J.W., 1994b. Toughness of an interface along a thin ductile layer joining elastic solids. Philos. Mag. A 70, 641–656.
Tvergaard, V., Hutchinson, J.W., 1996. On the toughness of ductile adhesive joints. J. Mech. Phys. Solids 44, 789–800.